Detection of OG:A lesion mispairs by MutY relies on a single His residue and the 2-amino group of 8-oxoguanine

Andrea J. Lee[†]*, Chandrima Majumdar[‡], Scott D. Kathe[†], Robert P. Van Ostrand[‡], Holly R. Vickery[‡], April M. Averill[†], Shane R. Nelson[§], Amelia H. Manlove[‡], Morgan A. McCord[†], Sheila S. David[‡*]

[†]Department of Microbiology and Molecular Genetics, University of Vermont, 95 Carrigan Drive, Burlington, VT 05405

[§]Department of Molecular Physiology and Biophysics, University of Vermont, 149 Beaumont Avenue, Burlington, VT 05405

[‡]Department of Chemistry, University of California, Davis, One Shields Avenue, Davis, CA 95616

KEYWORDS DNA repair, DNA damage, base excision repair, SM Fluorescence, DNA glycosylase, 8-oxoguanine, ROS.

ABSTRACT: MutY glycosylase excises adenines misincorporated opposite the oxidatively damaged lesion, 8-oxo-7,8-dihydroguanine (OG), to initiate base excision repair and prevent G to T transversion mutations. Successful repair requires MutY recognition of the OG:A mispair amidst highly abundant and structurally similar undamaged DNA base pairs. Herein we use a combination of *in vitro* and bacterial cell repair assays with single molecule fluorescence microscopy to demonstrate that both a C-terminal domain histidine residue and the 2-amino group of OG base are critical for MutY detection of OG:A sites. These studies are the first to directly link deficiencies in MutY lesion detection with incomplete cellular repair. These results suggest that defects in lesion detection of human MutY (MUTYH) variants may prove predictive of early onset colorectal cancer known an MUTYH-associated polyposis. Furthermore, unveiling these specific molecular determinants for repair makes it possible to envision new MUTYH-specific cancer therapies.

One of the most insidious DNA lesions is 8-oxo-7,8-dihydroguanine (OG) (Fig. 1A) due to its ability to form promutagenic OG:A mismatches during DNA replication. MUTYH plays a crucial role in preventing OG-associated G to T transversion mutations by excising A from OG:A mismatches, thereby initiating base excision repair (BER).[1–4] Inherited functionally compromised MUTYH variants are associated with a colorectal cancer predisposition syndrome known as MUTYH associated polyposis (MAP), which is characterized by an accumulation of G to T transversions in *APC* and other tumor suppressor genes.[5,6] Arguably, the most crucial step for initiation of MUTYH-mediated repair is proper recognition and discrimination of rare OG:A mismatches over highly abundant and structurally similar canonical DNA base pairs (bp) (Fig. 1).

Structure activity relationships determined for bacterial MutY with modified OG:A substrates have indicated that damage detection and processing occurs in multiple stages and may differ for *in vitro* assays that utilize short oligonucleotides when compared with cellular assays using longer plasmid-based substrates.[7,8] In these studies, modifications to the 8-oxo position of OG significantly decreased *in vitro* kinetics and lesion affinity, while removal of the 2-amino group of OG (8-oxoinosine, 8OI, Fig. 1D) only modestly impacted these parameters. In contrast, MutY-mediated cellular repair of a damage-containing plasmid was found to be highly sensitive to any modification of the OG structure, including removal of the 2-amino group. These differences led us to propose that the 2-amino group of OG is required for initial detection and recognition of OG:A lesions - a process that is more demanding in the context of excess undamaged DNA in cells. Notably, the base pairing of A with OG in the *syn* conformation projects the 2-amino group into the major groove of the DNA helix resulting in a unique structural signature of the OG:A lesion distinct from canonical bps (Fig. 1A-C).[7]

The sensitivity of MutY repair to the 8OI substitution suggests that specific structural motifs in MutY serve as "sensors" of interhelical OG:A bps through interactions with the 2-amino group of OG. In recent X-ray structural studies of *Geobacillus stearothermophilus* (*Gs*) MutY, we uncovered the importance of a highly conserved $H_{305}XFSH_{309}$ loop within the C-terminal domain that tucks into the major groove proximal to the OG (Fig. 1E).[9,10] Modeling using several *Gs* MutY structures[9-11] suggests that H309 (H296 in *E. coli*) may be appropriately positioned to detect the 2-amino group of OG_{syn} (Fig S1). In the current study, we employed a combination of single molecule (SM) fluorescence microscopy DNA search assays, *in vitro* glycosylase and binding measurements, and a plasmid based cellular repair assay to investigate the search and repair behavior of *E. coli* WT and H296A MutY on OG:A and 8OI:A damage sites. Our results show that both elements are crucial for identifying and repairing the OG:A lesion.

In order to probe the roles of the 2-amino group and H296 residue on MutY activity, adenine glycosylase assays were

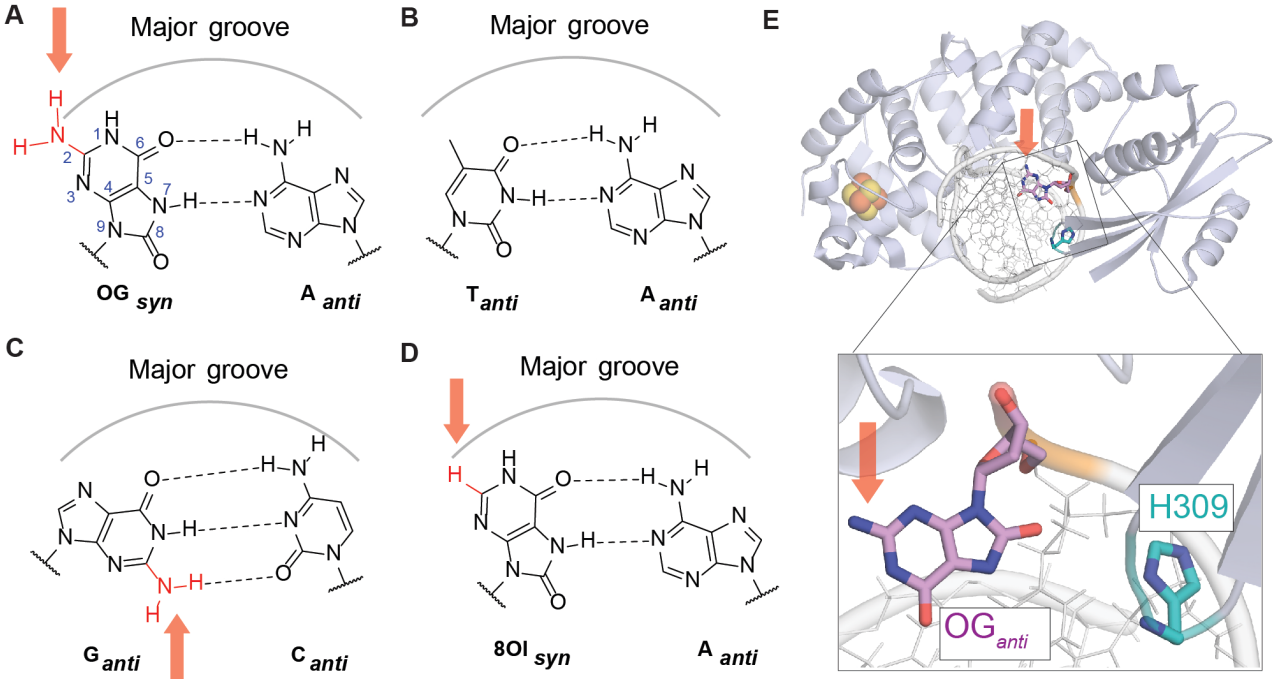

Figure 1: Recognition of OG:A through 2-amino group of OG and MutY HXFSH loop. OG_{syn}:A_{anti} mispairs (A) place the 2-amino group in the DNA major groove, providing a structural signature distinct from other bps, such as T:A (B) or G:C (C); removal of the 2-amino group of OG provides 8OI (D). Crystal structure of *Gs* MutY bound to the TS analog, OG:1N (PDB ID 6U7T), shows rotation of OG from *syn* to *anti* and extrusion of A into the active site following lesion recognition (E).[10] The HXFSH loop (teal) protrudes into the helix with H309 (H296 in *E. coli* MutY) proximal to OG_{anti} (purple) Inset (E). Rotation of OG_{anti} to OG_{syn} for the interhelical OG:A would position the 2-amino group more closely to H309.

performed using 30 bp DNA duplexes containing a central OG:A or 8OI:A bp with WT or H296A MutY. The rate constants (k_2) of adenine excision by WT or H296A MutY were measured under single turnover (STO, [E] > [DNA]) conditions (Fig. 2A, S2). Dissociation constants (K_D) for OG:A and 8OI:A, also using 30 bp substrates, were measured using a catalytically inactive E37S MutY, and for WT and H296A MutY using a non-cleavable substrate analog OG:FA (where FA = 2'-deoxyfluoroadenosine) (Fig. S3).[12] Cellular lesion repair was determined by transformation of a lesion-carrying plasmid into *E. coli* expressing WT or H296A, or lacking MutY, followed by plasmid extraction and restriction digestion to measure conversion of the lesion to G:C (Fig. 2B).[7,8,13]

Remarkably, the results with H296A MutY acting on OG:A substrates *in vitro* and in cells mirrored those with WT MutY acting on 8OI:A substrates. Specifically, the adenine excision rate constant k_2 was decreased 2-fold in both scenarios (Fig. 2A, S2).[7] H296A MutY showed a significantly decreased (150-fold) binding affinity for an OG:FA duplex (K_D = 3 ± 1 nM) compared to WT MutY (K_D = 0.02 ± 0.01 nM; Fig. S3). This decrease is more dramatic than the 10-fold decrease observed in the case of 8OI:A (K_D = 0.04 ± 0.01 nM)[7] versus OG:A duplex (K_D <0.003 nM) with E37S MutY. Cellular repair with H296A MutY on OG:A is significantly less than WT on OG:A, and only slightly more than WT on 8OI:A (Fig. 2B).[7] These results imply that in the context of a large excess of undamaged DNA and rare OG:A lesions, H296A MutY was largely incapable of recognizing the mispair. The *in vitro* rate constant of adenine

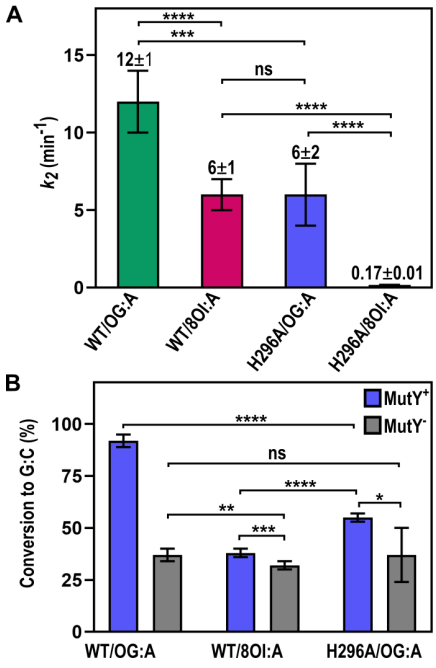

Figure 2: Mutation of H296 and removal of 2-amino group of OG impair MutY activity. (A) Mean adenine excision rates (k_2) of WT and H296A MutY on OG:A and 8OI:A[7] substrates. (B) Extent of WT or H296A MutY mediated repair as determined by conversion of OG:A or 8OI:A to G:C in *E. coli*. (error bars represent standard deviations; ns, p> 0.05; * p<0.05; ** p<0.01; ***p<0.001; ****p< 0.0001).

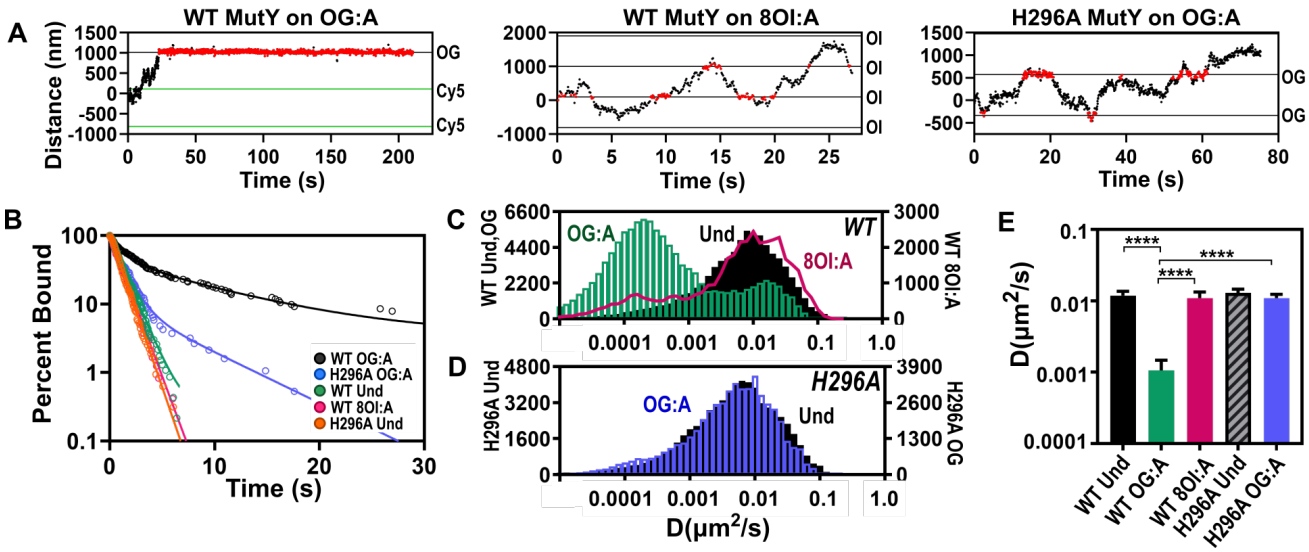

Figure 3: Single Molecule Studies of MutY Lesion Detection. (A) Representative displacement trajectories proximal to a lesion site marked in red (more trajectories in SI). (B) Residence time for binding to damage sites in DNA tightropes. Two exponential fits were used for WT MutY (1.4 ± 0.3 s (56%); 9.4 ± 2.7 s (44%); 152 events) and H296A (1.0 ± 0.09 s (87%); 5.9 ± 5.1 s (13%); 188 events) on OG:A. Single exponential fits were used for WT MutY on 8OI:A (1.1 ± 0.02 s, 241 events), WT MutY on undamaged (1.2 ± 0.04 s, 462 events), and H296A on undamaged (0.97 ± 0.02 s, 318 events). (C) Time-weighted sliding window analysis (60 frame window) for WT MutY on undamaged (black), OG:A (green), and 8OI:A concatemers (red trace). (D) Time-weighted analysis of diffusive behavior of H296A in the presence of OG:A (blue) and undamaged DNA concatemers (black). Y-axis shows total number of frames in C and D. (E) Mean value of trajectory-weighted diffusion constants of the conditions in C and D (error bars represent SEM, ****p<0.0001, two tailed).

excision for H296A MutY with the 8OI:A duplex was 35-fold reduced relative to the value observed for either modification with the WT enzyme or substrate (Fig. 2A, S2), indicating a synergistic interaction between H296 and the 2-amino group of OG.

In order to directly observe real-time damage search behavior of individual Qdot labeled WT and H296A MutY, we utilized SM DNA tightrope assays (Fig. S4). SM tightropes were up to 30 μm in length and contained a single damage site for every 2626 undamaged DNA base pairs (Fig. S4, S5). SM trajectories show paused displacement events for WT in the presence of OG:A sites (Fig. 3A, S4, S6), but noticeably fewer of these pauses for WT on 8OI:A sites (Fig. 3A, S4, S7) or H296A on OG:A sites (Fig. 3A, S4, S8).

Residence time at the damage site was measured for a subset of trajectories in which the position of the enzyme relative to damage sites could be mapped with reference to fiducial dye markers (Fig. 3B, Fig. S6-S8). These encounter lifetimes were then fit to a single exponential for WT and H296A MutY on undamaged DNA, and WT MutY on 8OI:A-containing DNA (Fig. 3B). Decay curves were fit to two exponentials for WT and H296A MutY on OG:A-containing DNA (Fig. 3B). The fast transit diffusion lifetimes for all five conditions are approximately 1s, within error of each other, and are consistent with the expected rate for random diffusion tracking along the DNA backbone (i.e. no recognition of a damage site).[14] Importantly, the single fast transit time observed in SM trajectories of WT MutY in the presence of 8OI:A damage sites indicates no significant pausing or recognition of the damage analog site and likely no catalysis in the context of the DNA tightrope. In contrast, WT MutY on OG:A forms a stable enzyme-damage complex in approximately half of the encounters. H296A MutY shows a small (13%) population of slow diffusion encounters with OG:A, suggesting some nominal recognition of damage sites consistent with the minimal repair of OG:A in cells. However, persistent H296A MutY pausing at damage sites is not shown in the time weighted diffusion histograms that describe overall H296A MutY behavior on OG:A (Fig. 3D) or in the overall binding lifetime data (Fig. S9). Overall binding lifetimes were fit using survival estimator methodologies as described by Kaplan and Meier (Fig. S9).[15] Only WT MutY on OG:A showed an overall binding lifetime that was significantly longer than lifetimes for the other conditions, and the bound fraction did not drop to zero at the maximum observation time (300s).

To characterize the diffusive behavior of all molecules for each SM condition, SM data were analyzed using time-weighted sliding window diffusion analysis (Fig. 3C, D).[14,16] This approach reveals diffusive behavior for all trajectories that persist for longer than 60 frames. In the absence of damage, WT MutY primarily scans rapidly along undamaged DNA tightropes at a rate consistent with random rotational diffusion along the DNA backbone (Dmax ~ 0.01 μm²/s) (Fig. 3C).[16,17] The presence of OG:A sites leads to a significant decrease in WT MutY diffusion to a rate consistent with pausing (Dmax < 0.001 μm²/s).[14,16] In the presence of 8OI:A, WT MutY shows primarily fast diffusion indicating no recognition of the damaged base analog (Fig. 3C). H296A MutY diffusion on undamaged DNA is almost

indistinguishable from WT MutY on undamaged tightropes. Similar to WT MutY on 8OI:A, H296A MutY shows almost no slow diffusion or pausing in the presence of OG:A (Fig. 3D). These results suggest that H296A MutY damage recognition events are rare and short-lived compared to WT MutY. Whole trajectory MSD analysis of diffusion constants resulted in mean values that corroborate the time-weighted diffusion analysis (Fig. 3E).

This work demonstrates that both the 2-amino group of OG and the MutY H296 are essential for detection of the OG:A bp in the context of large tracts of undamaged DNA, and MutY lesion detection deficiencies lead to failed overall repair of OG:A in cells. *In vitro* adenine cleavage assays are less sensitive to changes in these sensor features. Although removal of the 2-amino or H296 decreased adenine excision rates only 2-fold, the cumulative effect of removing both decreased the rate of A excision by almost two orders of magnitude implying interdependence of the two features. One potential sensing mechanism involves initial pausing of MutY via a steric clash between H296 and the 2-amino group of OG. Alternatively, the influence of the two features on each other may be more subtle, and result from altered conformational flexibility of the HXFSH loop. After pausing, additional interactions between the His and adjacent residues mediated by electrostatics or H-bonding may in turn trigger a cascade of conformational changes leading to base pair opening and adenine insertion in the active site. The sensitivity of MutY to a single change in the HXFSH loop suggests a yet unrecognized class of MUTYH recognition domain variants that may play a role in increased transversion mutations leading to carcinogenesis.

The HXFSH loop is located far from the active site pocket or DNA intercalation loop of MutY and is a unique structural feature to MutY homologs. The unexpected importance of the two singular positions of H296 and the 2-amino of 8OI for lesion detection points to a novel approach to develop allosteric inhibitors for MUTYH.[9] Inhibitors for MUTYH would be useful chemical biology probes and may potentially serve as cancer chemotherapeutics to reduce cancer cell proliferation or associated inflammatory responses. [18-21]

ASSOCIATED CONTENT

Supporting Information

The Supporting Information including detailed materials and methods, *in vitro* product production curves for glycosylases and binding isotherms, and SM trajectories and analyses is available free of charge on the ACS Publications website.

AUTHOR INFORMATION

Corresponding Author

*Authors to whom correspondence should be addressed:
A.J.L.: andrea.lee@med.uvm.edu, S.S.D.:
ssdavid@ucdavis.edu

Author Contributions

All authors have given approval to the final version of the manuscript.

Funding Sources

The work was supported by grants from the NIH CA067985 and NSF CHE1905304 (S.S.D.) and NIH CA P01098893 (A.J.L.). A.H.M. was a predoctoral trainee supported by T32-GM008799 from NIGMS-NIH. A.H.M. was also supported by GAANN and Corson-Dow fellowships. M.A.M. was supported by the Distinguished Undergraduate Summer Research Award from UVM.

ABBREVIATIONS

ROS, reactive oxygen species; SM, single molecule; BER, base excision repair; MAP, MUTYH associated polyposis; bp, base pairs; OG, 8-oxo-7,8-dihydroguanine; WT, wild type.

REFERENCES

(1) Banda, D. M.; Nuñez, N. N.; Burnside, M. A.; Bradshaw, K. M.; David, S. S. Repair of 8-OxoG:A Mismatches by the MUTYH Glycosylase: Mechanism, Metals and Medicine. Free Radic. Biol. Med. 2017, 107, 202–215. https://doi.org/https://doi.org/10.1016/j.freeradbiomed.2017.01.008.

(2) Krishnamurthy, N.; Muller, J. G.; Burrows, C. J.; David, S. S. Unusual Structural Features of Hydantoin Lesions Translate into Efficient Recognition by Escherichia Coli Fpg. Biochemistry 2007, 46 (33), 9355–9365. https://doi.org/10.1021/bi602459v.

(3) Nakabeppu, Y. Regulation of Intracellular Localization of Human MTH1, OGG1, and MYH Proteins for Repair of Oxidative DNA Damage. Prog Nucleic Acid Res Mol Biol 2001, 68, 75–94.

(4) Manlove, A. H.; Nuñez, N. N.; David, S. S. The GO Repair Pathway: OGG1 and MUTYH. In The Base Excision Repair Pathway; WORLD SCIENTIFIC, 2016; pp 63–115. https://doi.org/10.1142/9789814719735_0003.

(5) Al-Tassan, N.; Chmiel, N. H.; Maynard, J.; Fleming, N.; Livingston, A. L.; Williams, G. T.; Hodges, A. K.; Davies, D. R.; David, S. S.; Sampson, J. R.; Cheadle, J. P.;. Inherited Variants of MYH Associated with Somatic G : C -> T : A Mutations in Colorectal Tumors. Nat. Genet. 2002, 30 (2), 227–232. https://doi.org/Doi 10.1038/Ng828.

(6) Raetz, A. G.; David, S. S. When You're Strange: Unusual Features of the MUTYH Glycosylase and Implications in Cancer. DNA Repair (Amst). 2019, 80, 16–25. https://doi.org/https://doi.org/10.1016/j.dnarep.2019.05.005.

(7) Manlove, A. H.; McKibbin, P. L.; Doyle, E. L.; Majumdar, C.; Hamm, M. L.; David, S. S. Structure–Activity Relationships Reveal Key Features of 8-Oxoguanine: A Mismatch Detection by the MutY Glycosylase. Acs Chem. Biol. 2017, 12 (9), 2335–2344. https://doi.org/10.1021/acschembio.7b00389.

(8) Livingston, A. L.; O'Shea, V. L.; Kim, T.; Kool, E. T.; David, S. S. Unnatural Substrates Reveal the Importance of 8-Oxoguanine for in Vivo Mismatch Repair by MutY. Nat. Chem. Biol. 2008, 4 (1), 51–58. https://doi.org/Doi 10.1038/Nchembio.2007.40.

(9) Peyton Russelburg, L.; L. O'Shea Murray, V.; Demir, M.; R. Knutsen, K.; L. Sehgal, S.; Cao, S.; S. David, S.; P. Horvath, M. Structural Basis for Finding OG Lesions and Avoiding Undamaged G by the DNA Glycosylase MutY. ACS Chem. Biol. 2019, 15 (1), 93–102. https://doi.org/10.1021/acschembio.9b00639.

(10) Woods, R. D.; O'Shea, V. L.; Chu, A.; Cao, S.; Richards, J. L.; Horvath, M. P.; David, S. S. Structure and Stereochemistry of the Base Excision Repair Glycosylase MutY Reveal a Mechanism Similar to Retaining Glycosidases. Nucleic Acids Res. 2016, 44 (2), 801–810. https://doi.org/10.1093/nar/gkv1469.

(11) Wang, L.; Chakravarthy, S.; Verdine, G. L. Structural Basis for the Lesion-Scanning Mechanism of the MutY DNA Glycosylase. J. Biol. Chem. 2017, 292 (12), 5007–5017. https://doi.org/10.1074/jbc.M116.757039.

(12) Nuñez, N. N.; Majumdar, C.; Lay, K. T.; David, S. S. Chapter Two - Fe–S Clusters and MutY Base Excision Repair Glycosylases: Purification, Kinetics, and DNA Affinity Measurements. In Fe-S Cluster Enzymes Part B; Academic Press, 2018; Vol. 599, pp 21–68. https://doi.org/https://doi.org/10.1016/bs.mie.2017.11.035.

(13) Majumdar, C.; Nuñez, N. N.; Raetz, A. G.; Khuu, C.; David, S. S. Chapter Three - Cellular Assays for Studying the Fe–S Cluster Containing Base Excision Repair Glycosylase MUTYH and Homologs in Fe-S Cluster Enzymes Part B Academic Press, 2018; Vol. 599, pp 69–99. https://doi.org/https://doi.org/10.1016/bs.mie.2017.12.006.

(14) Nelson, S. R.; Kathe, S. D.; Hilzinger, T. S.; Averill, A. M.; Warshaw, D. M.; Wallace, S. S.; Lee, A. J. Single Molecule Glycosylase Studies with Engineered 8-Oxoguanine DNA Damage Sites Show Functional Defects of a MUTYH Polyposis Variant. Nucleic Acids Res. 2019, 47 (6), 3058–3071. https://doi.org/10.1093/nar/gkz045.

(15) Kaplan, E. L.; Meier, P. Nonparametric Estimation from Incomplete Observations. J. Am. Stat. Assoc. 1958, 53 (282), 457–481. https://doi.org/10.1080/01621459.1958.10501452.

(16) Lee, A. J.; Warshaw, D. M.; Wallace, S. S. Insights into the Glycosylase Search for Damage from Single-Molecule Fluorescence Microscopy. DNA Repair (Amst). 2014, 20, 23–31. https://doi.org/10.1016/j.dnarep.2014.01.007.

(17) Dunn, A. R.; Kad, N. M.; Nelson, S. R.; Warshaw, D. M.; Wallace, S. S. Single Qdot-Labeled Glycosylase Molecules Use a Wedge Amino Acid to Probe for Lesions While Scanning along DNA. Nucleic Acids Res. 2011, 39 (17), 7487–7498. https://doi.org/10.1093/nar/gkr459.

(18) Visnes, T.; Cázares-Körner, A.; Hao, W.; Wallner, O.; Masuyer, G.; Loseva, O.; Mortusewicz, O.; Wiita, E.; Sarno, A.; Manoilov, A.; Astorga-Wells, J.; Jemth, A.-S.; Pan, L.; Sanjiv, K.; Karsten, S.; Gokturk, C.; Grube, M.; Homan, E. J.; Hanna, B. M. F.; Paulin, C. B. J.; Pham, T.; Rasti, A.; Berglund, U. W.; von Nicolai, C.; Benitez-Buelga, C.; Koolmeister, T.; Ivanic, D.; Iliev, P.; Scobie, M.; Krokan, H. E.; Baranczewski, P.; Artursson, P.; Altun, M.; Jensen, A. J.; Kalderén, C.; Ba, X.; Zubarev, R. A.; Stenmark, P.; Boldogh, I.; Helleday, T. Small-Molecule Inhibitor of OGG1 Suppresses Proinflammatory Gene Expression and Inflammation. *Science* **2018**, *362* (6416), 834 LP – 839. https://doi.org/10.1126/science.aar8048.

(19) Casorelli, I.; Pannellini, T.; De Luca, G.; Degan, P.; Chiera, F.; Iavarone, I.; Giuliani, A.; Butera, A.; Boirivant, M.; Musiani, P.; Bignami, M. The Mutyh Base Excision Repair Gene Influences the Inflammatory Response in a Mouse Model of Ulcerative Colitis. *PLoS One* **2010**, *5* (8), e12070. https://doi.org/10.1371/journal.pone.0012070.

(20) Sharbeen, G.; Youkhana, J.; Mawson, A.; McCarroll, J.; Nunez, A.; Biankin, A.; Johns, A.; Goldstein, D.; Phillips, P. MutY-Homolog (MYH) Inhibition Reduces Pancreatic Cancer Cell Growth and Increases Chemosensitivity. *Oncotarget* **2017**, *8* (6), 9216–9229. https://doi.org/10.18632/oncotarget.13985.

(21) Visnes, T.; Grube, M.; Hanna, B. M. F.; Benitez-Buelga, C.; Cázares-Körner, A.; Helleday, T. Targeting BER Enzymes in Cancer Therapy. DNA Repair (Amst). 2018, 71, 118–126. https://doi.org/https://doi.org/10.1016/j.dnarep.2018.08.015.

Table of Contents artwork